System Modeling and Simulation in 5G: A Hybrid Beamforming Approach With Power Flux Equalization in the Elevation Plane

Salman, Salman; Aslan, Yanki; Puskely, Jan; Roederer, Antoine; Yarovoy, Alexander

DOI
10.23919/EuMC.2019.8910782

Publication date
2019

Document Version
Final published version

Published in
2019 49th European Microwave Conference, EuMC 2019

System Modeling and Simulation in 5G: A Hybrid Beamforming Approach With Power Flux Equalization in the Elevation Plane

Salman Salman[#1], Yanki Aslan[#2], Jan Puskely[#3] Antoine Roederer[#4] Alexander Yarovoy[#5]

[#]MS3 Group, Department of Microelectronics, Faculty of EEMCS, Delft University of Technology, The Netherlands

[1]Salman@student.tudelft.nl, {[2]Y.Aslan, [3]J.Puskely-1, [4]A.G.Roederer, [5]A.Yarovoy}@tudelft.nl

***Abstract*— This paper presents a 5G downlink system model for a hybrid multi-user beamforming technique at the base station. The presented technique employs power flux equalization in the elevation plane using a fixed analog cosecant-shaped beam and digital beamforming in the azimuth plane. The system performances of various beamforming algorithms are investigated via Monte-Carlo simulations by creating simultaneous co-frequency beams towards the randomly-located users. The simulation results show that the proposed cosecant subarray hybrid beamforming statistically performs better than the state-of-the-art hybrid beamforming techniques and provides reduced complexity.**

***Keywords*— 5G, cosecant radiation pattern, hybrid beamforming, millimeter waves, multiuser communication.**

I. Introduction

In order to understand the feasibility of achieving the performance goals (number of simultaneous users, re-use of frequency spectrum, data rate per user, maximum distance for reliable communication etc.) with certain limitations (aperture size, number of antenna elements, power amplifier capabilities etc.), it is important to model the behaviour of integrated 5G antennas in the complete communication systems. Current studies on the link budget of 5G networks are still very limited in literature [1], [2] and there is lack of practical factors that should be considered in the overall design.

Incorporating the channel and propagation aspects in the antenna design has recently gained remarkable attention with the growing interest in 5G systems. A cascaded impedance-matrix model has been proposed in [3] to derive the requirements on base station antennas depending on the given channel model and beamforming algorithm. In [4], a base station antenna topology has been optimized for a statistically obtained current distribution along the aperture. Impact of array layout on the system performance has been investigated in [5], [6] in terms of average SINR and throughput. In [7], the effect of angular spacing of users on the interference-nulling performance has been investigated. In [8], it has been stated that the traditional array design criteria such as directivity and SLL are not representatives of 5G channel capacity and even grating lobes might be useful to increase the channel gain. In [9], it has been shown that generating a single beam towards the strongest multipath may outperform generating multiple beams (with reduced gain) in terms of carrier-to-interference-noise ratio unless there are several equally-strong multipaths. All these examples strongly indicate the importance of assessing the system performance in combination with the design of antennas and beamforming, which will be the main focus of the discussions in the paper.

In this paper, a novel system model is proposed for the recently introduced 5G base station antenna arrays with a cosecant radiation pattern in the elevation plane (see Fig. 1) and a low-complexity 1D digital beamforming in azimuth plane [10]. Existing mm-wave channel matrix formulation techniques are exploited and several beamforming approaches are studied via Monte-Carlo simulations, with a critical discussion on their statistical performance in terms of the cumulative distribution function (CDF) of the SINR at the users. The rest of the paper is organized as follows: Section II describes the system model and scenario. Section III discusses the simulation results. Section IV presents the conclusions.

II. System Model

We consider a base station (BS) antenna array of M elements (subarrays), serving K randomly picked single antenna user equipment's (UEs) in a cell sector on the ground with uniformly distributed users over the area. The BS serves all K UEs using space division multiple access (SDMA) in the same time and frequency sub-band, as shown in Fig. 2. We focus on the downlink (DL) scenario for data transmission. It is worthy to note that in this study, the propagation between BS and UEs is assumed to consist of only a single line-of-sight (LoS) path or a single dominant non-line-of-sight (NLoS). However, the analysis can be extended to other scenarios by incorporating more complex channel models.

A. Formulation of the performance metrics

The data symbols for transmission are generated by modulating generated data bits and then applying linear precoding using a certain beamforming technique (see Fig. 3). The symbols are normalized before being transmitted via M elements of the BS to the intended UEs. Let x be the combination of the modulated symbols intended for transmission to K users. The symbol for the k^{th} user is q_k with $E\{||q_k||^2\} = 1$. The precoded signal is given as

$$x = \sqrt{\alpha} W q \tag{1}$$

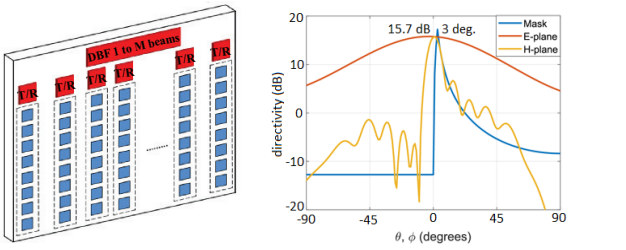

(a) (b)

Fig. 1. 5G cosecant subarray beamforming [10], (a) uniform linear array of subarrays (b) cosecant-square power distribution in elevation.

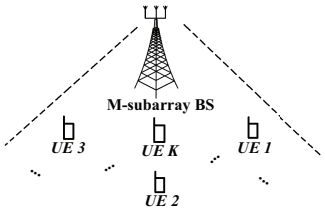

Fig. 2. A multi-user SDMA system in a cell sector with K number of active users sharing same frequency sub-band simultaneously and served by the BS with M subarrays.

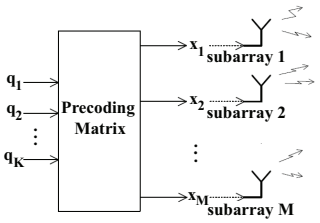

Fig. 3. Linear precoding architecture at the BS consisting of M subarrays and serving K simultaneous co-frequency users using SDMA.

where $q = [q_1 q_2 ... q_K]^T$ is the symbol vector, $W \in C^{MxK}$ is the precoding matrix with the beamforming vectors and α is the normalization factor satisfying the power constraint $E\{||x||^2\} = 1$. The normalization constant is computed as

$$\alpha = \frac{1}{E\{tr(WW^H)\}} \tag{2}$$

where the symbol $(^H)$ denotes the conjugate transpose. The received signal $y_{dl,k}$ at the k^{th} user in a cell from M element BS antenna array is given by

$$y_{dl,k} = \sqrt{\alpha SNR_k} h_k w_k q_k + \sqrt{\alpha SNR_k} \sum_{k' \neq k}^{K} h_k w_{k'} q_{k'} + z_k \tag{3}$$

where SNR_k is the signal-to-noise-ratio at the k^{th} user equipment, h_k is the k^{th} row of the channel matrix, and $H \in C^{KxM}$ is as formulated in the next section. w_k is the k^{th} column of the precoding matrix, W and z_k is the additive white Gaussian noise vector with zero mean and unit variance. The term $\sqrt{\alpha SNR_k} h_k^T w_k q_k$ in (3) shows the intended signal at the k^{th} user end while the term $\sqrt{\alpha SNR_k} \sum_{k' \neq k}^{K} h_k^T w_{k'} q_{k'}$ represents the interference from the signals of the other users. The performance metric for evaluating the downlink performance is selected as the statistical SINR at the receivers. The SINR for the k^{th} user in the downlink is given in (4). The SNR is evaluated using the link budget formulated in (5).

$$SINR_k = \frac{\alpha SNR_k |h_k w_k|^2}{\alpha SNR_k \sum_{k' \neq k}^{K} |h_k w_k|^2 + 1} \tag{4}$$

$$SNR_k = P_t + G_{t,k} + G_r - L_k - P_n \tag{5}$$

In (5), P_t is the transmit power allocated to each user, $G_{t,k}$ is the transmit antenna gain towards the k^{th} user, G_r is the receive antenna gain of each user, L_k is the propagation path loss towards the k^{th} user, and P_n is the noise floor of the receivers. Monte-Carlo simulations are performed for randomly selected users in a cell sector and the cumulative distribution function (CDF) of the SINR for all users and for all random realizations is calculated, which enables to analyze the SINR performance of all users statistically. The SINR for different beamforming techniques is compared for the 5^{th} percentile SINR value (for which 95% of users have larger SINR than this value) as in [11].

The acheivable sum-rate (SR) for the downlink system is also given in (6) in terms of the calculated user SINRs.

$$SR = \sum_{k=1}^{K} E\{\log_2(1 + SINR_k)\} \tag{6}$$

B. *Formulation of the channel matrix*

The mm-wave domain is characterized by high free-space path loss and results in limited scattering and spatial selectivity. Besides, large arrays with closely spaced elements for multiuser massive MIMO communication in the mm-wave bands leads to high antenna correlation. This combination of dense arrays in a spatially selective scattering environment makes the traditional MIMO statistical fading analysis inaccurate for the mm-wave channel modeling. Therefore, a narrow-band clustered geometric channel model based on Saleh-Valenzuela model is generally adopted which enables to precisely capture the mathematical structure of mm-wave channels [12], [13]. The channel matrix H is the sum of the rays coming from N_{cl} clusters with each cluster contributing N_{ray} propagation paths to the channel. The k^{th} row of the discrete time narrow band channel $H_{(k,:)}$ for M antenna elements at BS and N element UE can be formulated as

$$H_{(k,:)} = \gamma \sum_{i,l} \alpha_{i,l}^k \Lambda_r(\phi_{i,l}^{r,k}, \theta_{i,l}^{r,k}) \Lambda_t(\phi_{i,l}^{t,k}, \theta_{i,l}^{t,k}) a_r(\phi_{i,l}^{r,k}, \theta_{i,l}^{r,k}) a_t(\phi_{i,l}^{t,k}, \theta_{i,l}^{t,k})^H \tag{7}$$

where γ is the normalization factor that satisfies

$$\gamma = \sqrt{\frac{MN}{N_{cl} N_{ray}}} \tag{8}$$

A nomenclature for channel model formulation is given in Table 1.

The array response vector for M element uniform linear array (ULA) aligned along the y-axis can written as

$$a_{ULAy}(\phi_k) = \frac{1}{\sqrt{M}} [1, e^{j\beta d \sin\phi_k}, ..., e^{j(M-1)\beta d \sin\phi_k}]^T \tag{9}$$

Table 1. Nomenclature for the channel model formulation

$\alpha_{i,l}^{k}$	complex gain for the l_{th} ray in the for i_{th} scattering cluster
$\phi_{i,l}^{r,k}(\theta_{i,l}^{r,k})$	azimuth (elevation) angles of arrival for l_{th} ray
$\phi_{i,l}^{t,k}(\theta_{i,l}^{t,k})$	azimuth (elevation) angles of departure for l_{th} ray
$\Lambda_t(\phi_{i,l}^{t,k}, \theta_{i,l}^{t,k})$	antenna element gain for transmitter
$\Lambda_r(\phi_{i,l}^{r,k}, \theta_{i,l}^{r,k})$	antenna element gain for receiver
$a_t(\phi_{i,l}^{t,k}, \theta_{i,l}^{t,k})$	normalized transmitter steering vector at azimuth (elevation) angle $\phi_{i,l}^{t,k}(\theta_{i,l}^{t,k})$
$a_r(\phi_{i,l}^{r,k}, \theta_{i,l}^{r,k})$	normalized receiver steering vector at azimuth (elevation) angle $\phi_{i,l}^{r,k}(\theta_{i,l}^{r,k})$
$\sigma_{\alpha,i}^{2}$	average power of the i_{th} cluster

Table 2. Model Parameters

Array type	Uniform linear array (ULA) of subarrays
Antenna element type in the sub-arrays	Patch
Number of sub-arrays	16
Substrate Thickness	0.508 mm
Substrate relative permittivity	2.2
Center frequency	28 GHz
Path loss exponent	2 (free space)
Sub-array spacing	0.5λ
Max. cell radius	200 meters
Azimuth angular coverage	$\pm$ 45 degrees
Base station height w.r.t. UEs	10 meters
Number of users	4 (simultaneous, co-frequency)
User selection strategy	Randomly picked from a uniform distribution within the sector on the ground
Inter-user azimuth separation (radians)	M*(λ/D) with M = 0.6, 0.8, 1, 1.2 and 1.4, D = array length in λ
Directivity of a cosecant sub-array ($D_{\max,cosec}$)	15.70 dB (at the cell edge, i.e. 3^o below horizon)
Power amplifier (PA) output	20 dBm (1 PA per subarray)
Cosecant sub-array pattern	$G(\theta_k, \phi_k) = 10^{(\frac{D_{max}}{20})} \frac{csc\ \theta_k}{\text{csc}3^o} \sqrt{\cos\phi_k}$
Directivity of a receiver	0 dB
Noise floor of a receiver	-80 dBm
Number of random realizations	1000

where $\beta = \frac{2\pi}{\lambda}$ and d is the element spacing in the antenna array. In this paper, only one dominant ray with one cluster is considered. The base station consists of M sub-arrays while each user is assumed to have an isotropic antenna. Therefore, the channel matrix of a user k, shown in (7), is reduced to (10). Similar analysis can be performed straightforwardly to extend the model with a modified channel matrix having multiple clusters with each cluster having multiple reflected rays.

$$H_{(k,:)} = \sqrt{M}\Lambda_t(\phi^{t,k}, \theta^{t,k}) a_t(\phi^{t,k}, \theta^{t,k})^H \tag{10}$$

C. Beamforming techniques

In this paper, three different beamforming techniques are applied, namely, adaptive beam steering (ABS), zero-forcing (ZF) and minimum mean square error (MMSE), as formulated in (11). Using ABS formulation, the performance of generating different grid-of-beams (GoB) with pre-defined beam codebooks is also investigated. Moreover, amplitude tapering is considered to see the impact of varying maximum SLLs on the system performance.

$$\boldsymbol{W_{(:,k)}} = \begin{cases} [1, e^{j\beta d \sin\phi_k}, ..., e^{j(M-1)\beta d \sin\phi_k}] & for\ ABS \\ (H_{(k,:)}^H H_{(k,:)})^{-1} H_{(k,:)}^H & for\ ZF \\ (H_{(k,:)}^H H_{(k,:)} + \frac{K}{SNR_k} I_K)^{-1} H_{(k,:)}^H & for\ MMSE \end{cases} \tag{11}$$

III. Results and Discussions

In this section, we present the numerical analyses. The model parameters are summarized in Table 2.

a) Investigation of the maximum SLL on the statistical SINR: Fig. 4 shows the SINR performance of adaptive beam steering without windowing and with amplitude tapering resulting in different max. SLLs of -15 dB, -20 dB, -25 dB, -30 dB, -35 dB and -40 dB for a min. inter-user angular spacing of $1.2(\lambda/D)$. As seen in Fig. 4, the statistical SINR increases while max. SLL decreases. This trend continues until a min. SLL value of -25 dB, beyond which any further decrease in SLL degrades the SINR. This is due to that fact that as the SLL decreases, beamwidth increases. Thus, statistically, for a max. SLL below a certain threshold (i.e. -25 dB in this case), the beamwidth becomes wide enough to cause a large interference to the adjacent users. This indicates that in our scenario, ABS with -25 dB max. SLL performs statistically the best among all the windowing functions investigated. Fig. 5 provides the sum-rate comparison of ABS, ABS with max. -25 dB SLL, ZF and MMSE for varying min. inter-user spacing. It is seen that the MMSE and ZF beamforming techniques can effectively cancel the inter-user interferences and perform better than the ABS and ABS with amplitude tapering. However, ABS-based techniques have much less complexity.

b) Study on Grid of Beams with different beam overlap levels: The Grid of Beams (GoB) is generated by using different cross over points between adjacent beams (i.e. dB down from the respective mainlobe) in the azimuth. The points selected are 1 dB, 2 dB (to study the impact of decreasing grid density) and 3.9 dB (this selection leads to mutually-orthogonal grid of beams). The cosecant power distribution in elevation is applied on the generated weights of the respective GoBs. In addition, an amplitude tapering is also applied on the weighting vectors to achieve max. SLL of -25 dB. Note that the amplitude tapering results in an increase in beamwidth and loss of orthogonality for 3.9 dB GoB. The analyses are carried out with randomly distributed UEs having inter-user azimuth separation at least $1.2(\lambda/D)$. The CDF of SINR's for all the GoBs is shown in Fig. 6. The statistical performance is evaluated at the 5^{th} percentile of the realizations. According to the results, 1 dB GoB with amplitude tapering performs the best among all with an SINR value of 10.73 dB, followed by 1 dB GoB, 2 dB GoB, 2 dB GoB with windowing, 3.9 dB GoB and 3.9 dB GoB with windowing having SINR values 9.10 dB, 8.64 dB, 6.14 dB, 5.32 dB and 0.51 dB, respectively.

c) Comparative system analysis of the proposed cosecant hybrid beamforming technique: The statistical SINR performance of the cosecant hybrid beamforming with different beamforming techniques in azimuth plane is compared here with a commonly used hybrid beamforming sparse precoding algorithm, namely, orthogonal matching pursuit (OMP) [14]. The CDFs of SINRs for the cosecant beamforming technique using ABS with amplitude tapering, 1 dB GoB with amplitude tapering, ZF or MMSE (having

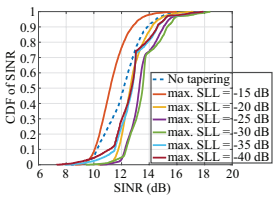

Fig. 4. Impact of max. SLL with amplitude tapering on the SINR performance for min. inter-user spacing of $1.2\lambda/D$.

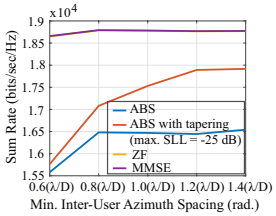

Fig. 5. Sum-rate for the cosecant sub-array antenna array for varying min. inter-user spacing.

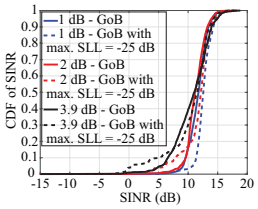

Fig. 6. Cumulative distribution function of SINR using Grid of Beams for 4 users with azimuth separation of at-least $1.2(\lambda/D)$.

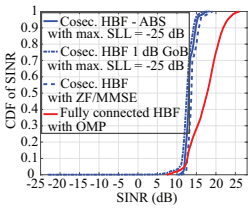

Fig. 7. Cumulative distribution function of SINR for randomly distributed users using various beamforming techniques with inter-user azimuth separation of at-least $1.2(\lambda/D)$.

identical results in this interference-dominated simulation) and the fully-connected HBF with OMP are presented in Fig. 7. For the 5^{th} percentile of the realizations, cosecant HBF with all of its azimuth beamforming techniques mentioned above performs better than fully-connected HBF with OMP. The cosecant HBF with ZF/MMSE performs the best among all at the 5^{th} percentile by outperforming cosecant HBF-ABS with tapering by 0.62dB, cosecant HBF-1dB GoB with tapering by 1.75dB and fully-connected HBF with OMP by 0.52dB. However, for the 10^{th} percentile of the realizations and above, the fully connected HBF with OMP outperforms all forms of cosecant HBF. This improvement of SINR at high percentiles is due to OMP's high degree of freedom as each RF chain is connected to every antenna element via a network of adders in the RF domain (with an order of magnitude more complexity).

IV. Conclusion

In this paper, a system model for a 5G downlink hybrid beamforming (HBF) technique has been presented by combining cosecant power flux equalization in the elevation plane and digital beamforming in the azimuth plane. The Saleh-Valenzuela geometric model is used for channel modeling with a single dominant path between BS and each UE. The Monte-Carlo simulations are performed with simultaneously served users sharing the same frequency sub-band and randomly located in a ground cell sector. The statistical SINR for all UEs is analyzed for all random realizations using the cumulative distribution function (CDF) with a certain threshold (i.e. the 5^{th} percentile of all the random realizations). The cosecant HBF topology performance has been studied using different azimuth beamforming techniques such as ABS, ABS with amplitude tapering, ZF and MMSE, along with the GoB approach. It was found out that the cosecant HBF with its all forms of azimuth beamforming outperforms the commonly used fully connected HBF with OMP algorithm for the 95 percent of the total random user position realizations while providing much reduced implementation and processing complexity. Under the ideal channel estimation and beamforming conditions, the cosecant HBF with ZF/MMSE performs the best among all the analyzed beamforming techniques.

Acknowledgment

This research was conducted as part of the NWO-NXP Partnership Program on Advanced 5G Solutions within the project titled "Antenna Topologies and Front-end Configurations for Multiple Beam Generation". More information: www.nwo.nl.

References

[1] "A straight path towards 5G," White Paper, Straight Path Communications Inc., Sept. 2015.

[2] Z. Pi and F. Khan, "An introduction to millimeter-wave mobile broadband systems," *IEEE Commun. Mag.*, vol. 49, no. 6, pp. 101–107, Jun. 2011.

[3] N. Amani, R. Maaskant, A. A. Glazunov, and M. Ivashina, "Network model of a 5G MIMO base station antenna in a downlink multi-user scenario," in Proc. 12th EuCAP, London, UK, Apr. 2018.

[4] C. Bencivenni, "Aperiodic array synthesis for telecommunications," Ph.D. dissertation, Dept. Elect. Eng., Chalmers Univ. of Tech., Gothenburg, Sweden, 2017.

[5] C. Bencivenni, A. A. Glazunov, R. Maaskant, and M. V. Ivashina, "Effects of regular and aperiodic array layout in multi-user MIMO applications," in *Proc. IEEE USNC/URSI NRSM*, San Diego, CA, USA, Jul. 2017.

[6] X. Ge, R. Zi, H. Wang, J. Zhang, and M. Jo, "Multi-user massive MIMO communication systems based on irregular antenna arrays," *IEEE Trans. Wireless Commun.*, vol. 15, no. 8, pp. 5287–5301, Aug. 2016.

[7] P. Wongchampa and M. Uthansakul, "Orthogonal beamforming for multiuser wireless communications: Achieving higher received signal strength and throughput than with conventional beamforming," *IEEE Antennas Propag. Mag.*, vol. 59, no. 4, pp. 38–49, Jun. 2017.

[8] G. Gottardi, G. Oliveri, and A. Massa, "New antenna design concept for future generation wireless communication systems," in Proc. 12th EuCAP, London, UK, Apr. 2018.

[9] V. Degli-Esposti, F. Fuschini, E. M. Vitucci, M. Barbiroli, M. Zoli, L. Tian, X. Yin, D. A. Dupleich, R. Muller, C. Schneider, and R. S. Thoma, "Ray-tracing-based mm-wave beamforming assessment," *IEEE Access*, vol. 2, pp. 1314–1325, Nov. 2014.

[10] J. Puskely, Y. Aslan, A. Roederer, and A. Yarovoy, "SIW based antenna array with power equalization in elevation plane for 5G base stations," in Proc. 12th EuCAP, London, UK, Apr. 2018.

[11] M. Giordani, M. Mezzavilla, A. Dhananjay, S. Rangan, and M. Zorzi, ""Channel Dynamics and SNR Tracking in Millimeter Wave Cellular Systems"," *CoRR*, vol. abs/1604.05623, 2016. [Online]. Available: http://arxiv.org/abs/1604.05623

[12] P. F. M. Smulders and L. M. Correia, "Characterisation of propagation in 60 ghz radio channels," *Electronics Communication Eng. J.*, vol. 9, no. 2, pp. 73–80, Apr 1997.

[13] H. Xu, V. Kukshya, and T. S. Rappaport, "Spatial and temporal characteristics of 60-ghz indoor channels," *IEEE J. Sel. Areas Commun.*, vol. 20, no. 3, pp. 620–630, Apr 2002.

[14] O. E. Ayach, S. Rajagopal, S. Abu-Surra, Z. Pi, and R. W. Heath, "Spatially sparse precoding in millimeter wave mimo systems," *IEEE Trans. Wireless Commun.*, vol. 13, no. 3, pp. 1499–1513, March 2014.